



GC/MS Analysis and Phyto-synthesis of Silver Nanoparticles Using *Amygdalus spinosissima* Extract: Antibacterial, Antioxidant Effects, Anticancer and Apoptotic Effects

Azadeh Farmahini Farahani ¹, Seyed Mohammad Mahdi Hamdi ^{1*}, and Amir Mirzaee ²

1. Department of Biology, Central Tehran branch, Islamic Azad University, Tehran, Iran

2. Department of Biology, Roudehen branch, Islamic Azad University, Roudehen, Iran

Abstract

Background: The present study was aimed at phyto-synthesized silver nanoparticles (AgNPs) using *Amygdalus spinosissima* (*A. spinosissima*) extract and to investigate the antibacterial, antioxidant effects, anticancer and apoptotic effects of phyto-synthesized AgNPs.

Methods: The bio-fabricated AgNPs were characterized using UV-visible spectroscopy (UV-visible), X-ray Diffraction (XRD), Fourier Transform Infrared (FTIR), Transmission Electron Microscopy (TEM), Scanning Electron Microscopy (SEM) and Energy Dispersive X-ray (EDX).

Results: The phyto-synthesized AgNPs showed maximum absorption in 438 nm, in the UV-visible spectrum. XRD peaks were observed at 2θ values in 38.20°, 44.40°, 64.60°, and 77.50° which are indexed as (111), (200), (220), and (311) bands of Face-Centered Cubic (FCC) structures of silver. FTIR analysis indicated that the AgNPs were capped with *A. spinosissima* extract. SEM and TEM micrographs revealed that the fabricated AgNPs were spherical and the average size range was 17.89 nm. Also, the EDX results show that the content of Ag was 90%.

Conclusion: The phyto-synthesized AgNPs had significant antibacterial activity against Gram-negative bacteria, as well as, the AgNPs exhibited great inhibitory effects on DPPH radicals and their antioxidant properties were favorably comparable to the antioxidant outcomes of ascorbic acid. Moreover, the AgNPs showed anti-cancer activity against the MCF-7 cell line with the IC₅₀=6.1 μg/ml. Moreover, the phyto-synthesized AgNPs could induce apoptosis in the MCF-7 cell line significantly. The GC-MS analysis of the *A. spinosissima* extract showed that 102 bioactive phyto-chemical compounds, which be of use to the synthesis of AgNPs.

Avicenna J Med Biotech 2022; 14(1): 79-88

Keywords: *Amygdalus spinosissima*, Anti-bacterial agents, Antioxidants, Apoptosis, Silver nanoparticle

* Corresponding author:
Seyed Mohammad Mahdi
Hamdi, Ph.D., Department of
Biology, Central Tehran branch,
Islamic Azad University, Tehran,
Iran
E-mail:
m.hamdi@iauctb.ac.ir
Received: 7 Apr 2020
Accepted: 24 May 2021

Introduction

Recently, nanoparticles have attracted researchers due to their many applications in drug delivery, microbial diseases and cancer management ^{1,2}. Due to their small size (1 to 100 nm), these structures have unique physicochemical and biological properties ³. Among nanoparticles, metal nanoparticles are synthesized by physical and chemical methods, which are very important ⁴. In chemical synthesis of metallic nanoparticles, chemical reducing agents including sodium hydrochloride and hydrazine can reduce the metallic ions into metallic nanoparticles ⁵. However, a small number of substances used in the chemical methods are toxic and dangerous and the synthesized nanoparticles

lack biocompatibility and it is always possible that they are not physiologically suitable for laboratory tests ⁶.

Despite all the studies on the antimicrobial properties of the extracts, which have made them very suitable for use, some stimulant and toxic properties have been found in them, which create many limitations in their use. Silver nanoparticles alone is toxic and carcinogenic and should be used with caution during testing. However, the aim of this study is to synthesize plants with silver nanoparticles, which is not harmful to the environment, but can be dangerous for the researcher during the experiment, which must be observed during safety tests ⁴. To overcome these prob-

lems, green synthesis or Phyto-synthesis methods are used in the fabrication of nanoparticles that are economically feasible and environmentally friendly ⁷.

In the Phyto-synthesis of metal nanoparticles, the plants extract is used as a reducing agent instead of toxic chemical compounds ⁸. The plants extract acts as a stabilizing agent in addition to its reducing properties ⁹. The synthesis of metal nanoparticles using plant extract is one-step and the plant extracts have secondary metabolites that can be caused by reducing properties ¹⁰. One of the metallic nanoparticles that are important in medical applications and today is synthesized by plant extracts is silver nanoparticles (AgNPs) ¹¹. So far, many plant extracts are used for the synthesis of AgNPs, but, in this study *Amygdalus spinosissima* (*A. spinosissima*) extract we used for the synthesis of AgNPs. In relation to previous studies, the synthesis of silver nanoparticles using European marjoram plant and its antimicrobial effects can be mentioned. In this study, European marjoram extract was used as a reducing agent for the biological production of silver nanoparticles and their study showed that silver nanoparticles had antimicrobial activity against gram-positive and negative bacteria ¹².

A. spinosissima is a species of tree native to Iran, Middle East and Central Asia, but widely cultivated elsewhere. *A. spinosissima* is a rich source of vitamin E, dietary fiber, B-vitamins, essential minerals mono-unsaturated fats and phytosterols which have cholesterol-lowering properties ¹³. Moreover, *A. spinosissima* has different biological properties including antibacterial, anticancer, antioxidant, antidiabetic, antiemetic, antihypertensive, hypoglycemic, hypolipidemic ¹⁴.

There were several reasons for choosing *A. spinosissima* in the present study. One of the useful areas for studying medicinal plants is to study their antimicrobial effects. As a result of the increasing use of antibiotics, many bacteria have become resistant to these drugs. Therefore, there is an urgent need to find new antimicrobial sources. And the use of medicinal plants for this purpose is a priority. Also, the effective antimicrobial compounds in them are less harmful to the consumer than antibiotics. Medicinal plants have also always been considered as chemical substitutes due to their ease of access, lower side effects, low toxicity and low cost ¹².

More studies have shown that the *Amygdalus* species are rich in tannins, phenols, flavonoids, carotenoids, and alkaloids, and it has been reported to show high antioxidant activities and that it can be considered as major factor for reducing silver to AgNPs ¹⁵. This study was aimed to synthesize silver nanoparticles AgNPs using *A. spinosissima* extract and to investigate the antibacterial, anticancer and apoptotic effects of synthesized AgNPs.

Materials and Methods

Plant collection and extract preparation

The fresh aerial parts and root of *Amigdalus spinosissima* (Bunge) French were obtained from the Iranian Biological Research Center (<http://www.en.ibrc.ir/>), and verified by Botanical Faculty (Herbarium no. 1391). To prepare the extract, the root and aerial parts of *A. spinosissima* were first placed in an air current and then completely dried in dark. 50 g of the powdered root and aerial parts, was added to 500 ml ethanol and distilled water solution for 12 hr and the resultant extract was stored at 4°C until used for the synthesis of AgNPs ¹⁶.

GC/MS analysis of *A. spinosissima* extract

The chemical composition of *A. spinosissima* extract was studied using a Gas Chromatography-Mass Spectrometer (GC/MS) system. GC/MS analysis was done on Shimadzu 15A gas chromatograph equipped with a split/spitless injector (250°C) and a flame ionization detector (250°C). Nitrogen was used as carrier gas (1 ml/min) and the capillary column used was a DB-5 (50 m 0.2 mm, film thickness 0.32 µm). The column temperature was kept at 60°C for 3 min and then heated to 220°C with a 5°C/min rate and kept constant at 220°C for 5 min. Relative percentage amounts were calculated from the peak area using a Shimadzu C-R4A Chromatopac, without the use of correction factors.

Phyto-synthesis and characterization of silver nanoparticles (AgNPs)

The AgNPs were phyto-synthesized by adding 100 ml of 1 mM silver nitrate with 5 ml of extract and incubated at room temperature for 30 min. After 45 min of reaction, the sediment was washed three times with distilled water by centrifugation at 13,000 rpm for 20 min, and the product was kept at 60°C for 2 hr ¹⁷. The absorption spectrum of prepared AgNPs was measured using a UV-vis spectrophotometer in the wavelength range of 200-700 nm. The dried powder of AgNPs was further analyzed by XRD (X-ray diffraction) and Fourier Transform Infrared spectrophotometer (FTIR). Size, shape, and morphology of the AgNPs were determined by Scanning Electron Microscopy (SEM) (XL30 electron microscope, Phillips, Japan) and Transmission Electron Microscopy (TEM) (Leo 906, TEM model 100 KV, Zeiss, Germany). The Energy-Dispersive X-ray Spectrometer (EDX) analysis was performed using the EDS X Sight Oxford instrument.

Radical Scavenging Activity (DPPH) Test

The free-radical scavenging activity test was performed using suspensions of the synthesized AgNPs at various concentrations as well as DPPH (1,1-diphenyl-2-picrylhydrazyl). A 0.1 mM solution of DPPH in methanol was prepared, and 1 ml of this solution was added to 3 ml of nanoparticle suspension with concentrations: 5, 25, 50, 100, and 200 µg/ml. The reaction mixture was then vortexed thoroughly and left in the dark at room temperature for 30 min whose absorbance was measured at 517 nm using a spectrophotometer.

The DPPH radical scavenging ability of the AgNPs

was calculated as:

$$\text{DPPH scavenging effect (\%)} = [(A_0 - A_1)/A_0] \times 100$$

Where, A₀ and A₁ represent the absorbance of the control and the sample, respectively. Subsequently, the concentration of AgNPs having a 50% radical scavenging activity was calculated and reported as IC₅₀. In addition, ascorbic acid was used as a positive control in this test.

Antibacterial activity of AgNPs

To evaluate the antimicrobial properties of the phyto-synthesized AgNPs, a Minimum Inhibitory Concentration (MIC) method was used. At first, 4 pathogenic bacteria including *Escherichia coli* (*E. coli*) ATCC 25922, *Salmonella enterica* ATCC 14028, *Staphylococcus aureus* ATCC 25923 and *Streptococcus pyogenes* ATCC 1447 were cultured in Luria-Bertani broth for 24 hr. The various concentrations of AgNPs including 100, 50, 25, 12.5, 6.25, 3.125 and 1.56 µg/ml was prepared and poured into the wells of the microplate. Subsequently, bacterial suspension with 0.5 McFarland concentration was added to each well. MIC is defined as the lowest concentration that inhibits microbial growth¹⁸. Besides, the Minimum Bactericidal Concentration (MBC) is considered the lowest concentration of an antibacterial agent required to kill selected bacteria.

MTT assay

The MTT [3-[4,5-dimethylthiazol-2-yl]-2,5-diphenyltetrazolium bromide] colorimetric method was used for determination of AgNPs cytotoxicity against breast cancer cell line (MCF-7). At first, 1×10⁴ cells were seeded into 96-well plates, followed by incubation in a CO₂ incubator at 37°C for 24 hr. The attached cells were treated with 100, 50, 25, 12.5, 6.25, 3.125, 1.56, 0.78 and 0.39 µg/ml concentrations of AgNPs for 24 hr. Subsequently, the MTT (Sigma Aldrich, Germany) was added into wells and the reaction mixture was kept at 37°C in a 5% CO₂ atmosphere for 4 hr. The MTT dye was then removed and all wells were dissolved using isopropanol. Finally, the absorbance of the samples was measured using an ELISA Reader (Organon Teknika, Netherlands) at 570 nm and the cell toxicity was determined using the following formula¹⁹:

$$\% \text{ Cell cytotoxicity} = 100 - \left[\frac{(A_t - A_b)}{(A_c - A_b)} \right] \times 100$$

$$\% \text{ Cell survival (viability)} = \frac{(A_t - A_b)}{(A_c - A_b)} \times 100$$

% Cell inhibition = 100-cell survival

A_t=Absorbance value of test compound

A_b=Absorbance value of blank

A_c=Absorbance value of control

Apoptosis/necrosis assay

The flow-cytometric method was used to determination of apoptosis in MCF-7 cells treated with AgNPs.

At first, 100,000 cells were treated with IC₅₀ concentration of AgNPs and untreated cells were used as controls. Finally, the apoptosis/necrosis assay was performed using the Annexin V/Propidium Iodide (PI) kit according to the instructions²⁰.

Apoptosis gene expression

Bax and *Bcl2* apoptosis genes expression were measured by Real-time qRT-PCR. Target gene expression levels were normalized to GAPDH as a house-keeping gene. The primers sequence of the target genes, including *Bax* and *Bcl-2*, and *GAPDH* (internal control), are given in table 1. Real-time qRT-PCR was performed independently in triplicate, for each of the different samples, and the data are presented as the mean values of the gene expression levels measured in the treated samples comparing to the controls²¹.

Statistical Analysis

All assays were conducted in triplicate and the obtaining data were analyzed using a one-way analysis of variance (ANOVA) with the post hoc test employing SPSS 17.0 software and the results were expressed as mean±standard deviation (SD) of three replicates. Moreover, p<0.05 was considered as significant.

Results

GC/MS analysis of *A. spinosissima* extract

Figure 1 shows the GC/MS analysis of all chemicals clarified in the *A. spinosissima* aerial part ethanolic extract. Based on table 1, 102 compounds were identified in the *A. spinosissima* extract. As mentioned earlier, *A. spinosissima* extract is full of polyphenolic compounds with different anti-oxidant, anti-cancer and anti-bacterial properties (Table 2)¹³. The biological activity of major phyto-components identified in the extract is shown in table 2. Because of reducing and capping agents of the main phytochemical constituents in *A. spinosissima* extract, a cap was formed around Ag⁺ of the bio-functionalized *A. spinosissima* AgNPs which was stable.

Phyto-synthesis and characterization of AgNPs

After 60 min of the reaction and change of reaction color, the ultraviolet spectroscopy analysis of AgNPs was evaluated using a UV-vis spectrophotometer between 200 and 700 nm. The absorption of AgNPs was observed in 375 nm wavelength in the UV-vis spectrum. Moreover, no additional peaks were seen in the spectrum, which showed a pure synthesis of AgNPs (Figure 2). Photograph of TEM shows that the synthesized AgNPs are spherical with 17.89 nm average size and to confirm the size of these nanoparticles, they were re-examined by DLS. In addition, the size and morphology of biosynthesized AgNPs using SEM revealed that the fabricated AgNPs had a spherical structure (Figure 3). The XRD patterns of phyto-synthesized AgNPs are shown in figure 4. In comparison with the cubic Ag reference pattern, the spectra data reveal the five diffraction lines (111), (200), (222), (311), and

GC/MS Analysis and Phyto-synthesis of Silver Nanoparticles

Table 1. Chemical composition of *A. spinosissima* extract

Number	Compound	RT (min)
1	Propenal dimethylhydazone	5.0364
2	p-xylene	5.6939
3	Ethylbenzene	6.1209
4	Benzaldehyde	7.5192
5	Nortricyclyl bromide	7.6306
6	Propanoic acid, 2-(aminoxy)	7.8645
7	Bicyclo[2.2.1]hept-2-ene, 1,7,7-trimethyl	8.4457
8	1,4-Cyclohexadiene, 1-methyl-4-(1-methylethyl)	9.1593
9	Bicyclo[3.1.0]hexan-2-ol, 2-methyl-5-(1-methylethyl)	9.3967
10	Benzaldehyde, 2,5-bis(trimethylsilyloxy)	9.6133
11	Benzeneacetonitrile, à-oxo-	9.7263
12	1,6-Octadien-3-ol, 3,7-dimethyl-, 2-aminobenzoate	9.8213
13	Bicyclo[3.1.0]hexan-2-ol, 2-methyl-5-(1-methylethyl)-(1a,2a,5a)	9.9166
14	Cyclopentasiloxane, decamethyl-	10.1652
15	Pyrazine, tetramethyl	10.2427
16	Bicyclo[3.1.0]hexan-2-ol, 2-methyl-5-(1-methylethyl)-(1a,2a,5a)	10.2782
17	4-Oxo-à-isodamascol	10.7658
18	Cyclobutane-1,1-dicarboxamide, N,N'-di-benzoyloxy	10.9157
19	1,3-Diacetyl-cyclopentane	11.1644
20	Decane, 3,7-dimethyl-	11.3076
21	3-Cyclohexene-1-methanol, à,à4-trimethyl-	11.3865
22	N-Benzyl-2-phenethylamine	11.8065
23	Benzothiazole	11.9656
24	Cyclohexasiloxane, dodecamethyl-	12.5870
25	1,3-Benzodioxole, 5-(2-propenyl)	12.7706
26	4-Hydroxy-2-methylacetophenone	13.0543
27	Eugenol	13.5943
28	à-Cubebene	13.9143
29	Decane, 6-ethyl-2-methyl	14.0766
30	Benzene, 1,2-dimethoxy-4-(2-propenyl)	14.1716
31	Vanillin	14.2648
32	1,4-Methanoazulene, decahydro-4,8,8-trimethyl-9-methylene-, 1S-(1a,3aa,4a,8aa)	14.4413
33	Caryophyllene	14.5266
34	Cycloheptasiloxane, tetradecamethyl-	14.7435
35	Phenol, 2-methoxy-4-(1-propenyl)	14.8579
36	1-Hexanone, 5-methyl-1-phenyl-	15.0107
37	Benzene, 1-(1,5-dimethyl-4-hexenyl)-4-methyl-	15.2070
38	Ethanone, 1-(3-hydroxy-4-methoxyphenyl)	15.3408
39	1,3-Cyclohexadiene, 5-(1,5-dimethyl-4-hexenyl)-2-methyl-, [S-(R*,S*)]	15.3728
40	Benzene, 1,2-dimethoxy-4-(1-propenyl)	15.3983
41	Benzoic acid, 4-hydroxy-3-methoxy-, methyl ester	15.6957
42	1,3-Benzodioxole, 4-methoxy-6-(2-propenyl)	15.7564
43	Benzene, 1,2,3-trimethoxy-5-(2-propenyl)	15.9854
44	Pentanoic acid	16.1181
45	Oxalic acid, isobutyl nonyl ester	16.5328
46	2-Naphthalenecarboxylic acid, 1-[(2-methylphenyl)imino]phenylmethoxy]-, methyl ester	16.6180
47	1-Heptadecyne	16.7414
48	Benzene, 1,2,3-trimethoxy-5-(2-propenyl)-	17.1645
49	Benzaldehyde, 4-hydroxy-3,5-dimethoxy	17.3703
50	Ar-tumerone	17.4008
51	Ethanone, 1-(2-hydroxy-4,6-dimethoxyphenyl)-	17.5227
52	Propanoic acid, 2,2-dimethyl-, 2,4-dinitrophenyl ester	17.6718
53	1-Heptadecyne	17.8852
54	4-Nonene, 3-methyl-, (Z)	17.9539
55	2,5,8-Triphenyl benzotriazole	18.3146
56	Tetradecanoic acid	18.3577
57	Tetradecanoic acid	18.3577
58	Benzoic acid, 4-hydroxy-3,5-dimethoxy-, hydrazide	18.5504
59	Ethanone, 1-(2,6-dihydroxy-4-methoxyphenyl)-	18.6079
60	3,4-Hexanedione, 2,2,5-trimethyl-	18.7416
61	Cyclopentene, 3-methyl-	18.9720
62	3-Hexadecyne	19.1175

Contd. Table 1. Chemical composition of *A. spinosissima* extract

Number	Compound	RT (min)
63	Methylenedioxyamphetamine, N, heptafluorobutyl deriv.	19.3373
64	3,7,11,15-Tetramethyl-2-hexadecen-1-ol	19.3690
65	3,7,11,15-Tetramethyl-2-hexadecen-1-ol	19.5607
66	2-Oxepanone, 7-butyl-	19.7201
67	1-Heptene, 1,3-diphenyl-1-(trimethylsilyloxy)	19.7810
68	n-Hexadecanoic acid	20.4091
69	n-Hexadecanoic acid	20.4091
70	Phthalic acid, 6-ethyl-3-octyl butyl ester	20.4169
71	5,7-Dihydroxy-4-methylcoumarin	20.8744
72	Silane, [[4-[1,2-bis[(trimethylsilyloxy)ethyl]-1,2-phenylene]bis(oxy)]bis(trimethyl-	21.1198
73	3,7-Bis[(trimethylsilyloxy)-9-methoxy-1-methyl(6H)dibenzo[b,d]pyran-6-one	21.4496
74	3,6-Dimethoxy-4-phenanthrol	21.6903
75	9,12-Octadecadienoic acid (Z,Z)-	22.0930
76	2,2'-Bioxirane	22.2873
77	Tetracosamethyl-cyclododecasiloxane	22.3315
78	Butyl citrate	22.4711
79	Phenanthrene, 7-ethenyl-1,2,3,4,4a,5,6,7,8,9,10,10a-dodecahydro-1,1,4a,7-tetramethyl-	22.6091
80	Silane, dimethyl(4-methoxyphenoxy)butoxy-	22.7851
81	1-Methylene-2b-hydroxymethyl-3,3-dimethyl-4b-(3-methylbut-2-enyl)-cyclohexane	22.9601
82	Podocarp-7-en-3-one, 13á-methyl-13-vinyl-	23.1399
83	3-Hexanone, 2,5-dimethyl	23.4607
84	Bicyclo[4.1.0]heptane, 7-pentyl	23.7909
85	3-Fluorophenol, triisobutylsilyl ether	23.9622
86	Acetic acid, (3,4-dimethoxyphenyl) (trimethylsilyloxy)-, methyl ester	24.1062
87	1-Methylene-2b-hydroxymethyl-3,3-dimethyl-4b-(3-methylbut-2-enyl)-cyclohexane	24.1663
88	1-Naphthalenecarboxylic acid, decahydro-1,4a-dimethyl-6-methylene-5-(3-methyl-2,4-pentadienyl)-, methyl ester.	24.3721
89	1-Methylene-2b-hydroxymethyl-3,3-dimethyl-4b-(3-methylbut-2-enyl)-cyclohexane	24.5667
90	1-Phenanthrenecarboxylic acid, 7-ethenyl-1,2,3,4,4a,4b,5,6,7,8,10,10a-dodecahydro-1,4a,7-trimethyl, methyl ester.	24.8974
91	1-Phenanthrenecarboxylic acid, 7-ethenyl-1,2,3,4,4a,4b,5,6,7,8,10,10a-dodecahydro-1,4a,7-trimethyl, methyl ester.	24.9021
92	1-Phenanthrenecarboxylic acid, 7-ethenyl-1,2,3,4,4a,4b,5,6,7,8,10,10a-dodecahydro-1,4a,7-trimethyl, methyl ester.	24.9146
93	1-Phenanthrenecarboxylic acid, 1,2,3,4,4a,9,10,10a-octahydro-1,4a-dimethyl-7-(1-methylethyl).	25.3226
94	Hexadecanoic acid, cyclohexyl ester	25.7714
95	Abietic acid	25.9857
96	Oxirane, tetradecyl-	26.3122
97	Phthalic acid, octyl 2-pentyl ester	26.3313
98	Octadecanoic acid	29.3581
99	Octadecanoic acid, octadecyl ester	29.3581
100	Isonipectic acid, N-allyloxycarbonyl-, tetradecyl ester	29.9293
101	Terephthalic acid, 4-octyl octyl ester	30.4461
102	Benzonitrile, 4-(5-butyl-2-pyrimidinyl)-	32.4490

Table 2. Antibacterial activity of Phyto-synthesized AgNPs against pathogenic bacteria

Bacteria	MIC ($\mu\text{g/ml}$)	MBC ($\mu\text{g/ml}$)
<i>Salmonella enterica</i>	62.5	125
<i>E. coli</i>	31.25	62.5
<i>S. Pyogenes</i>	50	100
<i>S. aureus</i>	100	100

(222) which are compatible with the standard pattern (Figure 5). EDX analysis was used to confirm the presence of elemental silver in Phyto-synthesized AgNPs (Figure 6). FTIR analysis of AgNPs shows the surface AgNPs of extract, which are considered as reducing and capping agent. The peak at 1222 cm^{-1} represents

C-N stretch. The peak at 1708 cm^{-1} shows C=O stretch. The peak at 2796 cm^{-1} represents H-C=O:C-H stretch (Figure 4).

DPPH Free-Radical Scavenging Assay

The antioxidant activity of the synthesized AgNPs was evaluated by DPPH radical scavenging assay, while ascorbic acid was used as a positive control. The AgNPs exhibited potential free radical scavenging activity (inhibitory concentration 50% [IC₅₀]=51.22 $\mu\text{g/ml}$). Note that the IC₅₀ value for ascorbic acid was 9.35 $\mu\text{g/ml}$.

Antibacterial activity of AgNPs

In this study, the MIC method was used to study the antibacterial activity of phyto-synthesized AgNPs. In

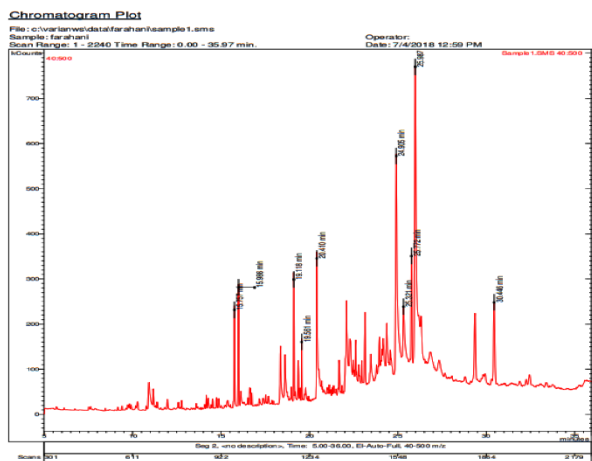


Figure 1. GC/MS chromatogram of *A. spinosissima* extract.

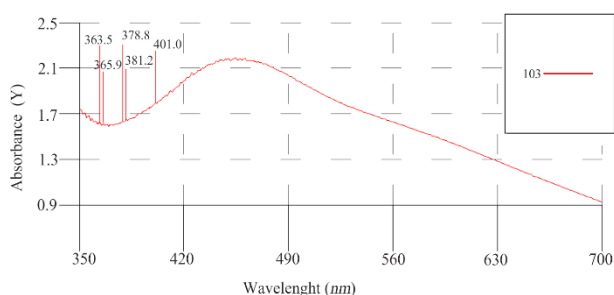


Figure 2. Ultraviolet-visible absorption spectra of phyto-synthesized AgNPs.

this test, pathogenic bacterial strains were treated with various concentrations of phyto-synthesized AgNPs including 0.78 to 100 $\mu\text{g/ml}$. The results of MIC and MBC showed that the biosynthesized AgNPs had the greatest effect against Gram-negative bacteria compared to Gram-positive bacteria (Table 2).

Cytotoxicity of AgNPs

The cytotoxicity of Phyto-synthesized AgNPs on MCF-7 cancer cells and L929 normal cells were evaluated using the MTT method and cell viability was measured after 24 hr. Treatment of both tumor and normal cell lines with various concentrations for 24 hr showed that the cytotoxicity of the synthesized AgNPs was dose-dependent while being less-toxic toward the L929 normal cell line. The results demonstrated that the bio-fabricated AgNPs exhibited the highest inhibitory effect on MCF-7 cells with $\text{IC}_{50}=6.1 \mu\text{g/ml}$ (Figure 7).

Apoptosis gene expression

Some molecular factors such as Bcl-2, Bax, casp3 and casp9 play a key role in the execution of apoptosis. Thus, to understand the molecular mechanism by which AgNPs induce apoptosis in MCF-7 cells, the expression ratios of Bax, Bcl-2, casp3 and casp9 genes in the MCF-7 cells treated with AgNPs were evaluated

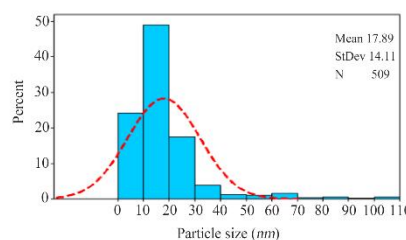
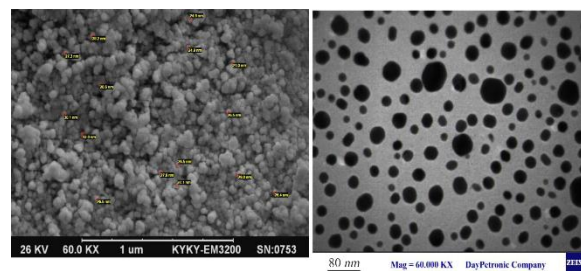


Figure 3. SEM and TEM images of phyto-synthesized AgNPs. Histogram of the particle sizes from TEM images.

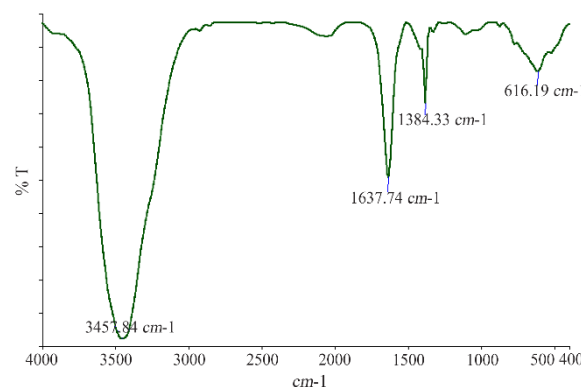


Figure 4. Fourier-transform infrared spectrum of phyto-synthesized AgNPs.

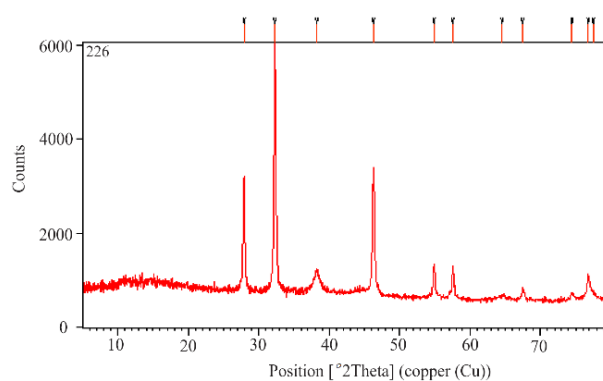
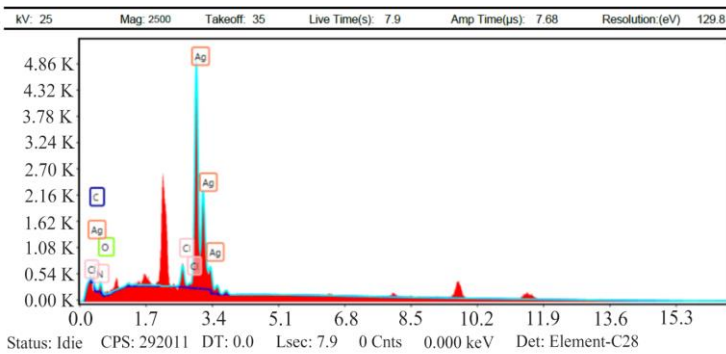


Figure 5. XRD analysis of phyto-synthesized AgNPs using *A. spinosissima* extract.

after 24 hr. Our results show that the expression of Bax, casp3 and casp9 genes, relative to the reference gene (GAPDH), was upregulated in the MCF-7 cells treated with AgNPs in 24 hr (3.26 ± 0.56 , 3.61 ± 0.67 and 3.92 ± 0.79 , respectively); whereas the expression of



eZAF smart quant results

Element	Weight %	Atomic %	Net Int.
CK	0.76	3.9	35.05
NK	0.01	0.03	0.13
OK	11.14	43.02	152.72
CIK	2.24	3.9	322.64
AqL	85.85	49.15	6011.9

Figure 6. Energy-dispersive X-ray (EDX) spectrum of green synthesized AgNPs. EDX spectroscopy study was employed to detect the existence of elemental silver.

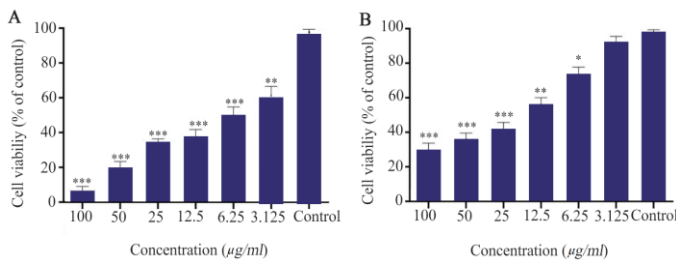


Figure 7. Cytotoxicity of phyto-synthesized AgNPs against MCF-7 (A) and L-929 (B) cell lines. (n=3; p<0.001***, p<0.01 **, p<0.05 *).

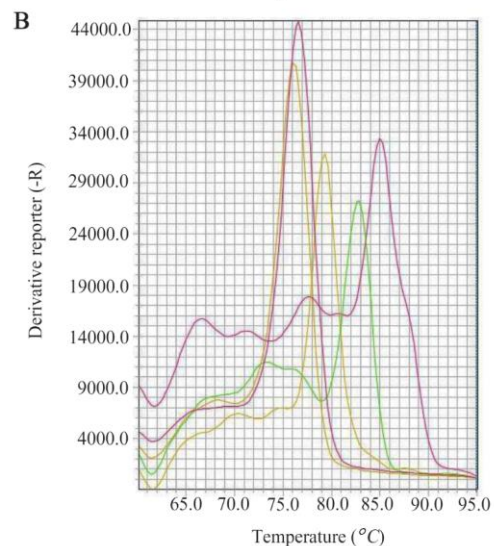
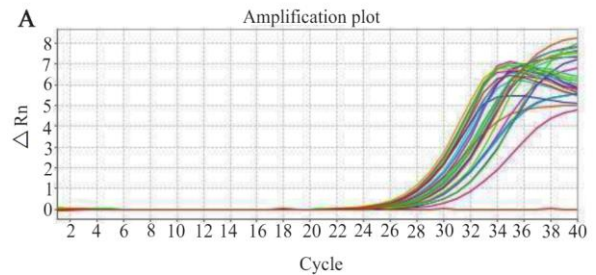


Figure 8. A) Amplification plot of *casp3*, *casp9*, *Bax* and *Bcl2* apoptosis related genes, B) melting curve of mention genes.

anti-apoptotic *Bcl-2* gene was significantly down-regulated (0.29 ± 0.44) in MCF-7 cells treated with AgNPs (Figures 8 and 9).

Apoptosis/necrosis assay

To determine apoptosis induction in MCF-7 cells treated with an IC50 concentration of the AgNPs, the MCF-7 cells were stained with FITC Annexin V and PI and analyzed using flow cytometry. During the initial phases of apoptosis, phosphatidylserine is transferred outside the cell membrane and is thus stained with Annexin V; whereas the PI stain is attached to the nucleus during necrosis. The flow cytometry results are shown in Figure 10, where the upper left square (Q1) indicates the percentage of late apoptotic cells and the upper right square (Q2) represents the percentage of cells with early apoptosis. As the results indicated, the phyto-synthesized AgNPs have led to 54.70% early apoptosis and 8.04% late apoptosis in the treated cells.

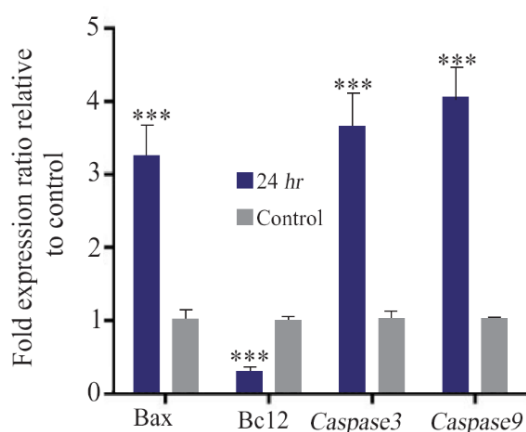


Figure 9. Apoptosis related genes expression analysis in MCF-7 cells treated with IC50 value of phyto-synthesized AgNPs. (n=3: p<0.001***, p<0.01**, p<0.05*).

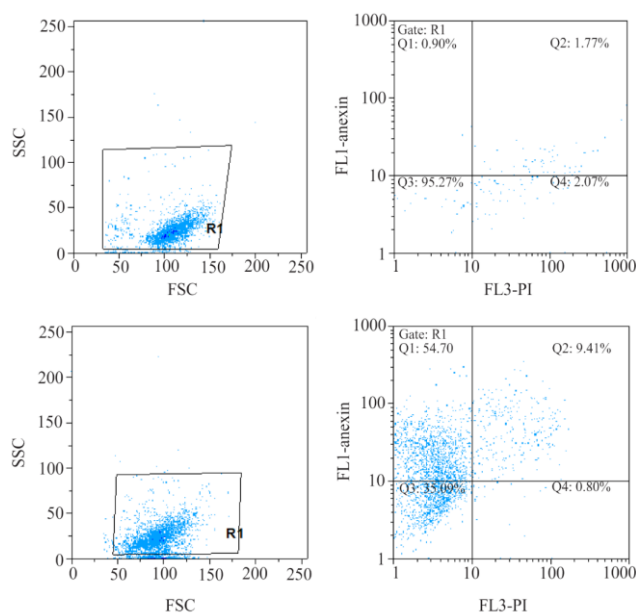


Figure 10. The flow-cytometric analysis of MCF-7 cells treated with phyto-synthesized AgNPs. The bottom left square: live cells, top left square: early apoptosis, bottom right square: necrosis, upper right square: delayed apoptosis.

Discussion

Recently, plant extracts are widely used for the green biosynthesis of nanoparticles. Compared with micro-organisms as reducing agents, the use of plant extracts is fast, cost-effective, simple, non-pathogenic and convenient. Besides, the phytochemical compounds in the plant extract enhanced the activity of AgNPs. Among the secondary metabolites, polyphenols are considered as potent antioxidant compounds that capture the ability of free radicals. If polyphenols are high in plant extracts, it will increase its antioxidant properties and increase the intrinsic activity of AgNPs²¹.

In this study, we used the *A. spinosissima* extracts to synthesize AgNPs. The results also showed that synthesized AgNPs have significant antibacterial effects on Gram-negative bacteria so that AgNPs can alter the permeability of the cell membrane. Moreover, the AgNPs showed anticancer activity against the MCF-7 cell line with the IC₅₀=6.1 µg/ml. Moreover, the phyto-synthesized AgNPs could induce apoptosis in the MCF-7 cell line significantly.

So far, several studies have examined the green synthesis of nanoparticles using plant extracts. In 2009, in a study the interaction of silver nanoparticles with the anti-tumor drug Aminocaracidine 9 was performed on cells. They showed that silver nanoparticles could control the release of the aminocaracidine 9 in living cells. They found that silver nanoparticles could act as a liberating drug carrier²². In another study, Ahmed and his colleagues obtained a formulation and evaluation of azathioprine drug loaded on silver nanoparticles. Their method was green synthesis based on polysaccharides²³. Another study evaluated the loading of turmeric on silver nanoparticles for pharmacodynamics and antibacterial properties. The results of their research showed a high level of antibacterial properties²⁴.

The AgNPs were synthesized using *A. spinosissima* extract at 37°C, while other studies used high temperature and pressure to regenerate AgNPs. *A. spinosissima* extract has various phytochemicals that can reduce the silver ions. It was proposed that the phytochemical compounds containing hydroxide groups are responsible for the reduction of silver ions. Nanomaterials, and especially metallic nanomaterials, disable enzymes and DNA micro-organisms with electron equilibrium between electron donor groups such as thiol, carboxylate, amide, imidazole, endol, and hydroxyl due to their surface charge and surface-to-volume ratio. In this study, after 30 min of the addition of *A. spinosissima* extract, the silver ions were reduced and color changed, which represented the synthesis of AgNPs. The results of TEM and SEM showed that the phyto-synthesized AgNPs were spherical with 17.89 nm average size. In this study, two biological activities of AgNPs were studied: anti-microbial and cytotoxic activity. Antibacterial activity of phyto-synthesized AgNPs against pathogenic bacteria showed that AgNPs have significant antibacterial effects against studied pathogenic bacteria. Among these, *E. coli* and *Salmonella* were more sensitive to AgNPs comparing to others. More studies show that AgNPs have significant effects on Gram-negative bacteria comparing to Gram-positive bacteria²⁵.

One of the antibacterial mechanisms of AgNPs is the binding of AgNPs to the surface of the cell membrane that changed the permeability and cellular respiration. Another mechanism is the entrance of AgNPs inside the cell and the release of silver ions from AgNPs that bind to oxygen, sulfur, and nitrogen in functional biomolecules that lead to cell death²⁶. An-

other reason for more antimicrobial effects of AgNPs against Gram-negative bacteria is due to the lesser thickness of the peptidoglycan in Gram-negative bacteria²⁷.

Also, the results of this study showed that cytotoxicity of AgNPs is dose-dependent and it has significant effects on MCF-7 cancer cells compared to normal L-929 fibroblast cells. Till now, several studies have shown that AgNPs enter into cells through processes such as endocytosis, phagocytosis, and diffusion²⁸. Studies have also shown that the absorption of AgNPs depends on the cell type and the size of the nanoparticle²⁹. Miethling-Graff *et al* reported the size-dependent (10, 20, 40, 60, and 100 nm) effects of AgNPs in the human LoVo cell line³⁰.

Generally, cancer is one of the devastating diseases and its treatment is limited, but with the development of nanotechnology, the therapeutic application of AgNPs is under investigation³¹. Moreover, studies show that cancer cells are more sensitive to AgNPs than normal cells³². The AgNPs are effective in breast cancer, leukemia, hepatocellular carcinoma, skin and oral carcinoma³³. Finally, to investigate the mechanism by which AgNPs elicit cell apoptosis in a dose-dependent manner, Real-Time PCR was used in MCF-7 cells treated with an IC₅₀ concentration of AgNPs. Our findings indicated that the expressions of apoptosis-related genes were increased with AgNPs treatment. Previous research reported that many different NPs and nanomaterials can affect apoptosis-related genes, such as *Bax*, *casp3*, *casp9*, and *P53*³⁴. Therefore, our Real-Time PCR data suggest that the increased apoptosis of AgNPs-treated MCF-7 cells was at least in part mediated by the change of apoptosis gene expression. Moreover, the flow-cytometric data support the apoptotic effect of AgNPs in the MCF-7 cell line. The MCF-7 cells exposed to AgNPs significantly increased the late apoptotic and necrotic cells as compared with untreated control cells.

Conclusion

Generally, the results of this study showed that the phyto-synthesis of AgNPs are economical, eco-friendly and straightforward reproducible. The phyto-synthesized AgNPs had significant antibacterial activity against Gram-negative bacteria, as well as, the AgNPs exhibited great inhibitory effects on DPPH radicals and their antioxidant properties were favorably comparable to the antioxidant outcomes of ascorbic acid. Moreover, the AgNPs showed anticancer activity against the MCF-7 cell line with the IC₅₀=6.1 µg/ml. The phyto-synthesize AgNPs were characterized by UV-Visible, EDX, XRD, FTIR, SEM, TEM. In FTIR, several phytochemical compounds identified which responsible for the reduction of silver ions to AgNPs. The results also showed that synthesized AgNPs have significant antibacterial effects on Gram-negative bacteria so that AgNPs can alter the permeability of the cell mem-

brane. In addition, The phyto-synthesized AgNPs exhibited selective cytotoxicity toward the cancerous MCF-7 cell line when compared to their effect on the normal cell line tested, whereas, treatment of MCF-7 cells with AgNPs increases the expression of apoptosis genes including, *Bax*, *casp3*, and *casp9*. The GC-MS analysis of the *A. spinosissima* extract showed that 102 bioactive phytochemical compounds, which be of use to the synthesis of AgNPs. In conclusion, the results of this study indicate that phyto-synthesized AgNPs can be used to develop new therapeutic agents for cancer therapy.

Acknowledgement

The authors would like to thank Mrs Dameshghian for his support in the present research.

References

- De Jong WH, Borm PJA. Drug delivery and nanoparticles: applications and hazards. *Int J Nanomedicine* 2008; 3(2):133-49.
- Jătariu A, Peptu C, Popa M, Indrei A. Micro- and nanoparticles-medical applications. *Rev Med Chir Soc Med Nat Iasi* 2009;113(4):1160-9.
- Faraz A, Faizan M, Sami F, Siddiqui H, Pichtel J, Hayat S. Nanoparticles: biosynthesis, translocation and role in plant metabolism. *IET Nanobiotechnol* 2019;13(4):345-52.
- Roach KA, Stefaniak AB, Roberts JR. Metal nanomaterials: Immune effects and implications of physicochemical properties on sensitization, elicitation, and exacerbation of allergic disease *J Immunotoxicol* 2019;16(1):87-124.
- Jeevanandam J, Barhoum A, Chan YS, Dufresne A, Danquah MK. Review on nanoparticles and nanostructured materials: history, sources, toxicity and regulations. *Beilstein J Nanotechnol* 2018;9:1050-74.
- Zhang XF, Liu ZG, Shen W, Gurunathan S. Silver nanoparticles: synthesis, characterization, properties, applications, and therapeutic approaches. *Int J Mol Sci* 2016;17: 1534.
- Erdogan O, Abbak M, Demirbolat GM, Birtekocak F, Aksel M, Pasa S, et al. Green synthesis of silver nanoparticles via *Cynara scolymus* leaf extracts: The characterization, anticancer potential with photodynamic therapy in MCF7 cells. *PLoS One* 2019;14(6):e0216496.
- Sathishkumar P, Vennila K, Jayakumar R, Yusoff AR, Hadibarata T, Palvannan P, et al. Phyto-synthesis of silver nanoparticles using *Alternanthera tenella* leaf extract: An effective inhibitor for the migration of human breast adenocarcinoma (MCF-7) cells. *Bioprocess Biosyst Eng* 2016;39:651-9.
- Manosalva N, Tortella G, Cristina Diez M, Schalchli H, Seabra AB, Durán N, et al. *World J Microbiol Biotechnol* 2019 May 27;35(6):88.
- Masum MMI, Siddiq MM, Ali KA, Zhang Y, Abdallah Y, Ibrahim E, et al. Biogenic synthesis of silver nanoparticles using *Phyllanthus emblica* fruit extract and its in-

hibitory action against the pathogen *Acidovorax oryzae* strain RS-2 of rice bacterial brown stripe. *Front Microbiol* 2019;10:820.

11. Salari S, Esmailzadeh Bahabadi S, Samzadeh-Kermani A, Yosefzadei F. In-vitro evaluation of antioxidant and antibacterial potential of green synthesized silver nanoparticles using *Prosopis farcta* fruit extract. *Iran J Pharm Res* 2019;18(1):430-455.
12. Vallverdú-Queralt A, Regueiro J, Alvarenga JFR, Martínez-Huelamo M, Leal LN, Lamuela-Raventos RM. Characterization of the phenolic and antioxidant profiles of selected culinary herbs and spices: caraway, turmeric, dill, marjoram and nutmeg. *Food Sci Technol* 2015;35(1):189-95.
13. *Prunus amygdalus* Batsch. *Plants of the World Online*. Royal Botanic Gardens, Kew. Retrieved 1 April 2019.
14. BĀDĀM–Encyclopaedia Iranica. www.iranicaonline.org. Retrieved 25 May 2019. The *Amygdalus communis* (or *Prunus amygdalus*), though undoubtedly native to the Iranian land-mass, is seldom found in natural stands there today.
15. Bolling BW. Almond polyphenols: methods of analysis, contribution to food quality, and health promotion. *Comprehensive Reviews Food Science Food Safety* 2017;16:346-68.
16. Suman TY, Rajasree SR, Jayaseelan C, Mary RR, Gayathri S, Aranganathan L, et al. GC-MS analysis of bioactive components and biosynthesis of silver nanoparticles using *Hybanthus enneaspermus* at room temperature evaluation of their stability and its larvicidal activity. *Environ Sci Pollut Res Int* 2016 Feb;23(3):2705-14.
17. Manosalva N, Tortella G, Cristina Diez M, Schalchli H, Seabra AB, Durán N, et al. Green synthesis of silver nanoparticles: effect of synthesis reaction parameters on antimicrobial activity. *World J Microbiol Biotechnol* 2019;35(6):88.
18. Lee YJ, Song K, Cha SH, Cho S, Kim YS, Park Y. Sesquiterpenoids from *Tussilago farfara* flower bud extract for the eco-friendly synthesis of silver and gold nanoparticles possessing antibacterial and anticancer activities. *Nanomaterials (Basel)* 2019;9(6):819.
19. Al-Sheddi ES, Farshori NN, Al-Oqail MM, Al-Massarani SM, Saquib Q, Bioinorg R. Wahab R, et al. Anticancer potential of green synthesized silver nanoparticles using extract of *Nepeta deflersiana* against human cervical cancer cells (HeLa). *Bioinorg Chem Appl* 2018;2018:9390784.
20. Baharara J, Namvar F, Ramezani T, Mousavi M, Mohammad R. Silver nanoparticles biosynthesized using *Achillea biebersteinii* flower extract: apoptosis induction in MCF-7 cells via caspase activation and regulation of Bax and Bcl-2 gene expression. *Molecules* 2015;20(2):2693-706.
21. Marslin G, Siram K, Maqbool Q, Selvakesavan RK, Kruzka D, Kachlicki P, et al. Secondary metabolites in the green synthesis of metallic nanoparticles. *Materials (Basel)* 2018;11(6):940.
22. Inbathamizh L, Ponnu TM, Mary EJ. In vitro evaluation of antioxidant and anticancer potential of *Morinda pubescens* synthesized silver nanoparticles. *J Pharmacy Research* 2013;6(1):32-8.
23. Ahmed S, Ahmad M, Swami BL, Ikram S. A review on plants extract mediated synthesis of silver nanoparticles for antimicrobial applications: a green expertise. *J Adv Res* 2016;7(1):17-28.
24. Ravindra S, Mulaba-Bafubiandi AF, Rajinikanth V, Varaprasad K, Reddy NN, Raju KM. Development and characterization of curcumin loaded silver nanoparticle hydrogels for antibacterial and drug delivery applications. *J Inorganic Organometallic Polymers Materials* 2012;22(6):1254-62.
25. Gordienko MG, Palchikova VV, Kalenov SV, Belov AA, Lyasnikova VN, Poberezhnyi DY, et al. Antimicrobial activity of silver salt and silver nanoparticles in different forms against microorganisms of different taxonomic groups. *J Hazard Mater* 2019;378:120754.
26. Jin JC, Xu ZQ, Dong P, Lai L, Lan JY, Jiang FL, et al. One-step synthesis of silver nanoparticles using carbon dots as reducing and stabilizing agents and their antibacterial mechanisms. *Carbon* 2015;94:129-41.
27. Cittrarasu V, Balasubramanian B, Kaliannan D, Park S, Maluventhan V, Kaul T, et al. Biological mediated Ag nanoparticles from *Barleria longiflora* for antimicrobial activity and photocatalytic degradation using methylene blue. *Artif Cells Nanomed Biotechnol* 2019;47(1):2424-30.
28. Mariadoss AV, Vinayagam R, Vijayakumar S, Balupillai A, Herbert FJ, Kumar S, et al. Green synthesis, characterization and antibacterial activity of silver nanoparticles by *Malus domestica* and its cytotoxic effect on (MCF-7) cell line. *Microb Pathogen* 2019:103609.
29. Karuppaiya P, Satheeshkumar E, Tsay HS. Biogenic synthesis of silver nanoparticles using rhizome extract of *Dyosma pleiantha* and its antiproliferative effect against breast and human gastric cancer cells. *Mol Biol Rep* 2019;46:4725-34.
30. Miethling-Graff R, Rumpker R, Richter M, Verano-Braga T, Kjeldsen F, Brewer J, et al. Exposure to silver nanoparticles induces size- and dose-dependent oxidative stress and cytotoxicity in human colon carcinoma cells. *Toxicol In Vitro* 2014 Oct;28(7):1280-9.
31. Asghari F, Khademi R, Esmaili Ranjbar F, Veisi Malekshahi Z, Faridi Majidi R. Application of nanotechnology in targeting of cancer stem cells: a review. *Int J Stem Cells* 2019;12(2):227-39.
32. Liao C, Li Y, Tjong SC. Bactericidal and cytotoxic properties of silver nanoparticles. *Int J Mol Sci* 2019;20(2):449.
33. Khwaja Salahuddin S, Azamal H, Rifaqat A, Rao K. A review on biosynthesis of silver nanoparticles and their biocidal properties. *J Nanobiotechnology* 2018;16: 14.
34. Govender R, Phulukdaree A, Gengan RM, Anand K, Chuturgoon AA. Silver nanoparticles of *Albizia adianthifolia*: the induction of apoptosis in human lung carcinoma cell line. *J Nanobiotechnology* 2013;11:5-12.